Mean barotropic vorticity balance in the South Western Indian Ocean

P. Penven[1], P. Tedesco[1], J. Gula[1], C. Ménesguen[1]

[1]Université de Bretagne Occidentale, CNRS, IRD, Ifremer, Laboratoire d'Océanographie Physique et Spatiale (LOPS), IUEM, Brest, France

1. Introduction

In the context of a western boundary current regime, the ocean circulation in the South Western Indian Ocean (also known as the greater Agulhas Current System) is particularly rich and energetic (Lutjeharms, 2006). When reaching the East Coast of Madagascar, the South Equatorial Current splits into two western boundary currents: the East and North Madagascar Currents (Schott, 2009). After rounding the northern tip of the island, the North Madagascar Current splits again into two other branches, the southern one feeding the Mozambique Channel in the form of large anticyclonic rings (Halo et al., 2014a). Mesoscale eddies are also generated south of Madagascar (Halo et al., 2014b) and both turbulent regions feed the Agulhas Current along the east coast of southern Africa. As the strongest western boundary current of the southern hemisphere, the Agulhas Current transports 75 Sv (1 Sverdrup = 10^6 m^3 s^{-1}) (Beal et al., 2015). It retroflects south of the continent to form the eastward flowing Agulhas Return Current, joining the Antarctic Circumpolar Current (Lutjeharms, 2006). From the Agulhas Retroflection, about 15 Sv leaks into the South Atlantic Ocean mostly in the form of Agulhas Rings (Richardson et al., 2003), contributing to the return loop of the meridional overturning circulation with global climatic implications (Beal et al., 2011).

Although important progress has been achieved in the reproduction of the oceanic circulation in Ocean General Circulation Models (Danabasoglu et al., 2014), large biases still occur for the Agulhas Current region (see for a recent example Zhu et al., 2018; or Penven et al., 2010 for a review). Knowledge of the controls of the circulation in the region could facilitate a better representation of the system and its variability.

Western boundary currents were originally thought to be controlled by frictional (Stommel, 1948; Munk 1950) or inertial (Charney, 1955) processes. More recently, when looking at regions large enough to filter out non-linear terms in the barotropic vorticity balance, Hughes and de Cuevas (2001) have highlighted the importance of bottom topography for their adjustment. This dominance in bottom pressure torque is indeed valid for the Gulf Stream independently of model vertical grids, numerics or horizontal resolutions (Schoonover et al., 2016).

Although a barotropic vorticity balance has already been used to separate specific regions at global scale (Sonnewald et al., 2019), such large-scale approaches could not resolve he intricacies of the greater Agulhas Current System. Here, using online diagnostics in a regional high-resolution model of the South Western Indian Ocean, we illustrate the controls of a few selected dominant processes in the region.

2. Data and method

The regional numerical experiments are done using the Coastal and Regional Ocean COmmunity model (CROCO, Debreu et al., 2012), a recent evolution of ROMS (Shchepetkin & McWilliams, 2005). CROCO solves the hydrostatic primitive equations using a topographic following vertical coordinate and higher order numerical schemes. To reach a sufficient resolution in the Agulhas region, three levels of horizontal grids (1/4º, 1/12º and 1/36º resolution) are embedded into each other following a 2-way nesting approach (Debreu et al., 2012). GLORYS 1/4º oceanic reanalysis (Ferry et al., 2012) provides the lateral boundary conditions for the largest grid. The daily ERA-ECMWF's reanalysis (Dee et al., 2011) feeds a bulk formula for the surface boundary conditions. Relative winds are used to derive the wind stress for a more realistic stability of the Agulhas Retroflection (Renault et al., 2017). The experiments are run for 21 years, from 1993 to 2014, after 2 years of spin-up. Comparisons within situ observations and satellite altimetry show how this simulation is able to reproduce the structure and variability of the Agulhas Current (Tedesco et al., 2019).

Following Hughes and de Cuevas (2001), Gula et al. (2015), Schoonover et al., (2016), Sonnewald et al., (2019) and Le Corre et al. (2020), a barotropic vorticity balance in the presence of topography is derived by vertically integrating the momentum equations and taking the curl. Since we are here only looking at the mean circulation, this balance simplifies too:

$$\beta\overline{V} = \mathbf{J}(\overline{P_b}, h) - \overline{Adv} + \boldsymbol{\nabla} \times \frac{\overline{\boldsymbol{\tau}^{wind}}}{\rho_0} - \boldsymbol{\nabla} \times \frac{\overline{\boldsymbol{\tau}^{bot}}}{\rho_0}$$

where β is the meridional gradient of the Coriolis parameter, V the meridional transport, P_b the bottom pressure, h the bottom topography, *Adv* the non-linear advection terms, ρ_0 the reference density, τ_{wind} the wind stress and τ_{bot} the bottom drag. The overbar accounts for a temporal average over 1993-2014. To avoid aliasing, each individual term of the barotropic vorticity

balance (Equation 1) is derived at run time by vertically integrating and taking the curl for each term of the horizontal momentum equation (including the time tendency) has described by Gula et al. (2015). They are subsequently averaged over time. They are divided by β, so they are all consistent as contributors to a mean meridional transport [$m^2\ s^{-1}$].

3. Results

Figure 1 presents horizontal maps of the terms of the mean barotropic vorticity balance for the model zoom at 1/36º resolution (the 5 terms plus the addition of bottom pressure torque and advection terms: bottom left). A primary equilibrium is noticeable locally at small scale between the inertial terms (advection, Figure 1 – bottom middle) assuring a tendency of the flow to carry on along a straight path and bottom pressure torque (Figure 1 – top middle) inducing a constraint to follow topographic contours. This results in a small-scale oscillatory pattern when bottom currents are in presence of large slopes. These oscillations are also present (albeit with larger length scales) in the 1/4º and 1/12º runs.

Figure 1: Maps of the terms of the mean barotropic

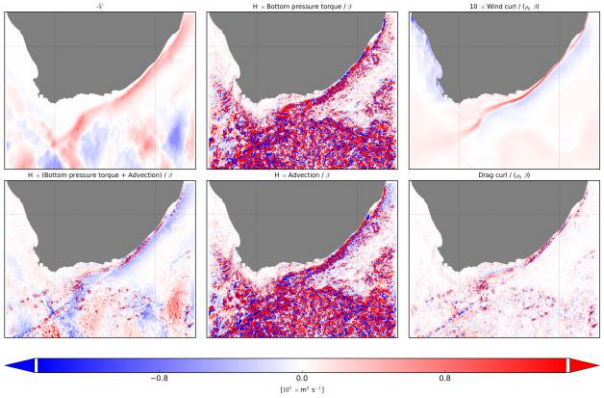

vorticity balance for the model zoom at 1/36º resolution. All terms are divided by β, so the units are consistent with a meridional transport ($m^2\ s^{-1}$). Note that the wind stress curl term is multiplied by 10.

Adding the 2 terms together allows the emergence of a larger scale inviscid balance for the Agulhas Current between advection of planetary vorticity (seen as a meridional transport in Figure 1 - top left) and the result of the addition (Figure 1 - bottom left).

As resolution increases (here seen at 1/36º), two new patterns arise. Firstly, although the wind stress curl is locally negligible at lower resolution, the current feedback on the wind stress results in a strip of positive curl along the inshore edge of the Agulhas Current (Figure 1 – top right; note here multiplied by 10). This could influence the shelf mean circulation. Secondly, *with increasing* resolution, bottom friction induces positive/negative patterns linked with topographic accidents such as seamounts, canyons, and shelf edges (Figure 1 – bottom right). They are directly balanced by bottom pressure torque and non-linear terms (Figure 1 – bottom left), with no significant influence on the meridional transport (Figure 1 – top left).

The terms presented in Figure 1 are averaged over specific regions of different characteristics, such as the Agulhas Current, the Agulhas Return Current, and, for lower resolution at larger scale, the Subtropical Southern Indian Ocean

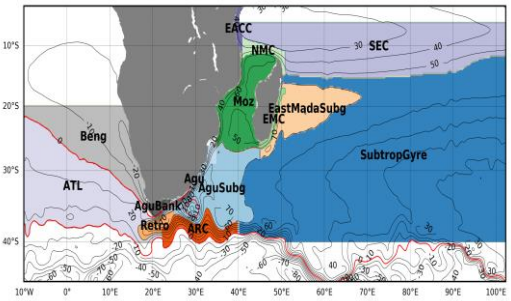

Figure 2: *Mean transport function (contours in Sverdrup; 1 Sv = 10^6 m^3 s^{-1}) from the larger scale simulation used to define the different regions (colors).*

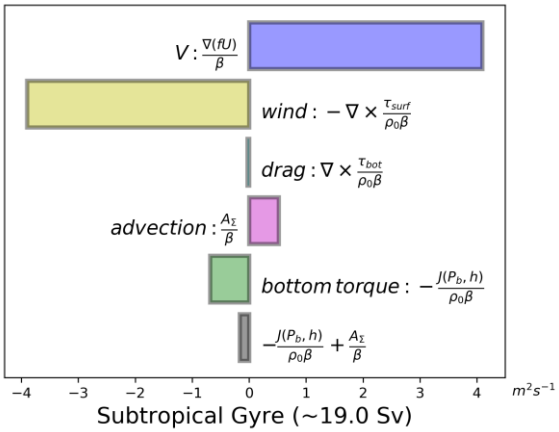

Figure 3: Mean barotropic vorticity balance over the southern Indian Ocean subtropical gyre (SubtropGyre region on Figure 2).

In the interior (east of 50ºE), the Subtropical Southern Indian Ocean is divided into two gyres separated by the South Equatorial Current (around 17ºS): the tropical gyre in the north (SEC of Figure 2) and the subtropical gyre in the south (SubtropGyre on Figure 2). For both gyres, the bottom pressure torque and non-linear terms are relatively small and cancel each other, leading to a quasi-Sverdrup balance (Wind stress curl ~ advection of planetary vorticity) with a net transport poleward for

the tropical gyre and equatorward for the subtropical gyre. Note that this results in the largest Sverdupian interior transport seen in the subtropical gyres of the world oceans (see for example Tomczak and Godfrey, 2003).

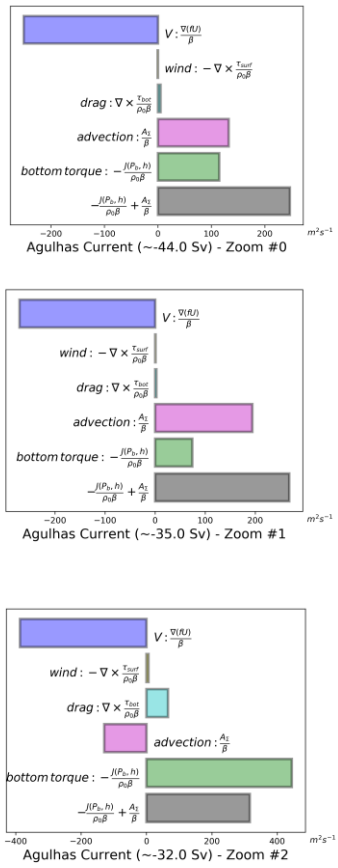

Figure 4: Mean barotropic vorticity balance over the Agulhas Current for the 1/4º (top), 1/12º (middle) and 1/36º (bottom) runs.

The inviscid control seen in other western boundary currents such as the Gulf Stream (Gula et al. ,2015; Schoonover et al., 2016) applies also to the Agulhas Current (Figure 4). Nonlinear advection acts in conjunction with bottom pressure torque in balancing the poleward transport in the 1/4º and 1/12º simulations, increasing with resolution. The role of advection appears reversed in the 1/36º run.

4. Conclusion

Here, using regional numerical simulations of the circulation in the South Western Indian Ocean, we have separated the different terms of the mean barotropic vorticity balance to assess their role in controlling the mean circulation in the region. A compensation occurs at small scale between advection and bottom pressure torque over the slopes. This appears to have an oscillatory pattern as seen by Le Corre et al. (2020) and is here directly dependent on the model resolution. Bottom friction also gains importance in general at higher resolution.

Nevertheless, a quasi-Sverdrup relation exists in the subtropical Indian Ocean. This confirms previous works which were using wind stress curl to explain changes in the incoming transports in the Agulhas Region (Rouault et al., 2009; Loveday et al., 2014).

As seen in other western boundary currents (Hughes and de Cuevas, 2001), the advection of planetary vorticity in the Agulhas Current itself is balanced by non-linear advection and bottom pressure torque. In contrast to the Gulf Stream (Schoonover et al., 2016), this balance presents a dependence to the resolution when comparing the 1/4º, 1/12º and 1/36º runs. This may be dependent on the region of integration, the mean structure of the current or it's variability. For the non-linear terms, we need to determine the role of eddies as done by Le Corre et al. (2020). This could also be important for the intensity of the recirculation loop just offshore of the Agulhas Current, east of the Agulhas Plateau. This loop can be exaggerated in some simulations (Penven et al., 2010).

Here just a few selected domains have been presented but others have contrasting dynamics such as the Agulhas Return Current (ARC on Figure 2) where the balance is controlled by advection and β terms (typical for standing Rossby waves) or the Benguela System and the Mozambique Channel dominated by passing large rings. This approach could also be extended as a framework for model inter-comparisons as proposed by the LEFE project AFRICA.

References

Beal, L. M., W. P. M. de Ruijter, A. Biastoch, R. Zahn, and the members of SCOR/WCRP/IAPSO Working Group 136 (2011), On the role of the Agulhas system in ocean circulation and climate, Nature, 472, 429–436.

Beal, L. M., S. Elipot, A. Houk, and G. M. Leber (2015), Capturing the transport variability of a western boundary jet: Results from the Agulhas Current Time-Series Experiment (ACT), J. Phys. Oceanogr., 45, 1302–1324.

Charney, J. G. (1955), The Gulf Stream as an inertial boundary layer, Proc. Natl. Acad. Sci. USA, 41, 731–740.

Danabasoglu, G., S. et al. (2014), North Atlantic simulations in Coordinated Ocean-ice Reference Experiments phase II (CORE-II). part I: Mean states, Ocean Model., 73, 76–107.

Debreu, L., P. Marchesiello, P. Penven, and G. Cambon (2012), Two-way nesting in split-explicit ocean models: algorithms, implementation and validation, Ocean Model., 49-50, 1–21.

Dee, D. P. et al. (2011), The ERA-Interim reanalysis: Configuration and performance of the data assimilation system, Quarterly Journal of the Royal Meteorological Society, 137, 553–597.

Ferry, N., L. et al. (2012), GLORYS2V1 global ocean reanalysis of the altimetric era (1992-2009) at meso scale, Mercator Ocean Quaterly Newsletter, 44, 28–39.

Gula, J., M. Molemaker, and J. McWilliams (2015), Gulf Stream dynamics along the Southeastern U.S. Seaboard, J. Phys. Oceanogr., 45, 690–715.

Halo, I., B. Backeberg, P. Penven, I. Ansorge, C. Reason, and J. Ullgren (2014a), Eddy properties in the Mozambique Channel: A comparison between observations and two numerical ocean circulation models, Deep Sea Res., Part II, 100, 38–53.

Halo, I., P. Penven, B. Backeberg, I. Ansorge, F. Shillington, and R. Roman (2014b), Mesoscale eddy variability in the southern extension of the East Madagascar Current: Seasonal cycle, energy conversion terms, and eddy mean properties, J. Geophys. Res., 119, 2014JC009820.

Hugues, C. W., and B. De Cuevas (2001), Why western boundary currents in realistic oceans are inviscid: A link between form stress and bottom pressure torques, J. Phys. Oceanogr., 31, 2871–2885.

Le Corre, M., J. Gula, and A. M. Tréguier (2020), Barotropic vorticity balance of the North Atlantic subpolar gyre in an eddy-resolving model, Ocean Sci., 16, 451–468.

Lutjeharms, J. R. E. (2006), The Agulhas Current, Springer-Verlag.

Munk, W. H. (1950), On the wind driven ocean circulation, J. Meteor., 7, 79–93.

Penven, P., S. Herbette, and M. Rouault (2010), Ocean modelling in the Agulhas current system, in Proceedings of the Joint Nansen-Tutu Scientific Opening Symposium and OceansAfrica Meeting, Nansen-Tutu Centre for Marine Environmental Research, pp. 17–21, Cape Town, South Africa.

Renault, L., J. C. McWilliams, and P. Penven (2017), Modulation of the Agulhas Current retroflection and leakage by oceanic current interaction, J. Phys. Oceanogr., 47, 2077–2100.

Schoonover, J., W. Dewar, N. Wienders, J. Gula, J. C. McWilliams, M. J. Molemaker, S. C. Bates, G. Danabasoglu, and S. Yeager (2016), North Atlantic barotropic vorticity balances in numerical models, J. Phys. Oceanogr., 46, 289–303.

Schott, F. A., S.-P. Xie, and J. P. McCreary (2009), Indian Ocean circulation and climate variability, Rev. Geophys., 47, RG1002.

Shchepetkin, A. F., and J. C. McWilliams (2005), The regional oceanic modeling system (ROMS): a split-explicit, free-surface, topography-following-coordinate oceanic model, Ocean Model., 9, 347–404.

Sonnewald, M., C. Wunsch, and P. Heimbach (2019), Unsupervised learning reveals geography of global ocean dynamical regions, Earth andSpace Science, 6, 784–794.

Stommel, H. (1948), The westward intensification of wind driven ocean currents, Trans. Amer. Geophys. Union, 29, 202–206.

Tedesco, P., J. Gula, C. Ménesguen, P. Penven, and M. Krug (2019), Generation of submesoscale frontal eddies in the Agulhas Current, J. Geophys. Res., 124, 7606–7625.

Tomczak, M., and J. S. Godfrey (2003), Regional Oceanography: an Introduction 2nd edn, 390 pp., Amer. Meteor. Soc.

Zhu, Y., B. Qiu, X. Lin, and F. Wang (2018), Interannual eddy kinetic energy modulations in the Agulhas Return Current, J. Geophys. Res., 123, 6449–6462